ELSEVIER

Journal of Chromatography A, 944 (2002) 77–91

JOURNAL OF CHROMATOGRAPHY A

www.elsevier.com/locate/chroma

Two-step solvent gradients in simulated moving bed chromatography
Numerical study for linear equilibria

Dorota Antos[a,b], Andreas Seidel-Morgenstern[a,c,*]

[a]*Max-Planck-Institut für Dynamik Komplexer Technischer Systeme, D-39120 Magdeburg, Germany*
[b]*Rzeszów University of Technology, Pl-35-959 Rzeszów, Poland*
[c]*Otto-von-Guericke-Universität Magdeburg, Universitätsplatz 2, P.O. Box 4120, D-39106 Magdeburg, Germany*

Abstract

The application of gradients in simulated moving bed (SMB) chromatography has recently attracted interest as a method for further improving the performance of this continuous separation process. One possible implementation of gradients consists in setting the solvent strength in the desorbent stream higher than that in the feed stream. As a result, the components to be separated are more retained in the zones upstream of the feed position and more easily eluted in the zones downstream of the feed position. If a liquid mobile phase is used, gradients can be created by dosing different solvents into the feed and desorbent ports. In a closed-loop gradient SMB arrangement the solvent strength within the unit will depend on the two feed compositions and on the characteristic flow-rates of the process. In this work an equilibrium stage model describing a true moving bed process is used to analyze numerically the main features of a two-step gradient SMB process. The adsorption isotherms are assumed to be always linear under isocratic conditions. The relevant Henry constants depend in a nonlinear manner on the composition of the solvent. Based on numerical simulations the impact of the two inlet solvent compositions is demonstrated in terms of the size and shape of regions of applicable flow-rates. Different strategies of designing the process are discussed and compared with respect to maximizing productivities and minimizing desorbent requirements.

Keywords: Gradient elution; Simulated moving bed chromatography; True moving beds; Adsorption isotherms; Mathematical modelling

1. Introduction

Recently, simulated moving bed (SMB) chromatography has increasingly attracted the attention of the chemical and pharmaceutical industries. The application of several periodically operated columns connected in series possesses advantages compared to classical batch chromatographic separations [1]. In particular, the concept offers the possibility to perform the separation in a continuous manner. Further, SMB processes have often proven to lead to higher productivities and lower solvent consumptions. Hitherto, the technology was mainly applied under isocratic conditions, i.e. the underlying distribution equilibria were permanently constant in all columns.

*Corresponding author. Otto-von-Guericke-Universität Magdeburg, Universitätsplatz 2, P.O. Box 4120, D-39106 Magdeburg, Germany. Tel.: +49-391-671-8644; fax: +49-391-671-2028.

E-mail address: anseidel@vst.uni-magdeburg.de (A. Seidel-Morgenstern).

0021-9673/02/$ – see front matter
PII: S0021-9673(01)01365-6

In contrast, it is well known from the experience available from analytical chromatography that modulation of the elution strength during the chromatographic process can be used efficiently to reduce cycle times and to increase sample throughputs [2].

The application of gradients to SMB processes with a supercritical eluent was introduced in Refs. [3,4]. The concept is based on using different pressures in the four characteristic SMB zones. This results in locally different mobile-phase densities and retention characteristics of the component to be separated. The zone responsible for desorption of the more-retained component can be operated at the highest density of the mobile phase, while the zone responsible for adsorption of the less-retained component can be operated at the lowest density level. This approach offers considerable potential to improve the process performance with respect to productivity and product concentration. Useful criteria to specify suitable operating conditions of an SMB process with a supercritical eluent were derived on the basis of equilibrium theory [5]. Recently, the effects of locally changing pH (pH gradients, [6]) and temperature (temperature gradients, [7]) on the performance of SMB processes were also analyzed.

In Ref. [8] the implementation of gradients using two different solvents at the two inlet ports was suggested. The feed is dosed continuously in a relatively weak solvent, whereas a stronger solvent is used as the desorbent. Thus, in the classical four-zone closed-loop SMB process, two distinct internal solvent composition levels exist which are separated by the two inlet positions. These two characteristic solvent strengths can be adjusted by using different amounts of a suitable modifier in the two feed streams. The first results of studying this type of two-step gradient SMB process demonstrate its potential to reduce significantly the solvent consumption and thus to increase product concentrations [8–10].

To design and optimize the SMB process working under isocratic conditions there is now a well-developed theory available to specify the relevant operating parameters, which are mainly the characteristic flow-rates (e.g., Refs. [11,12]). In contrast, not much systematic work has been done in order to analyze the described two-step gradient process where the solvent compositions in the two feed streams need to be specified as two additional parameters.

It is well known that the analysis of SMB processes can be considerably simplified by using models quantifying the steady state of analogous true moving bed (TMB) processes [1]. Based on this fact, in the present work a simple equilibrium stage model describing a two-step gradient TMB process was used to perform extensive numerical calculations in order to evaluate the potential of applying solvent gradients. An essential purpose of the study was to analyze the impact of the two additional parameters that need to be specified, in addition to the parameters required to design the conventional isocratic SMB process. The results are mainly summarized by presenting regions of acceptable flow-rates leading to specified purities of the two outlet streams. This approach has been proven to be very instructive in order to estimate process productivities and solvent consumptions under optimized isocratic conditions. For the idealistic situation of infinite stages, the equilibrium theory allows us to calculate analytically flow-rate regions leading to pure raffinate and extract streams [11,12]. This elegant approach was recently extended to analyze the two-step gradient process under linear conditions [10].

The numerical analysis presented here will be restricted to linear isotherms for a constant solvent composition. To describe the dependence of the Henry constants on the changing solvent compositions a nonlinear expression frequently used in analytical chromatography will be adopted. To test the numerical algorithm applied to solve the proposed stage model, a first prediction of the isocratic process for high efficiencies and pure product streams will be compared with the available corresponding analytical solution following from equilibrium theory. Subsequently, the impact of different solvent concentrations in the two inlet streams will be discussed systematically. In this analysis the influence of lower efficiencies and reduced purity requirements on the size and shape of the regions of applicable flow-rates will also be considered. Another objective of the study is to compare different possible constraints that might be chosen in specifying suitable regions of operating parameters.

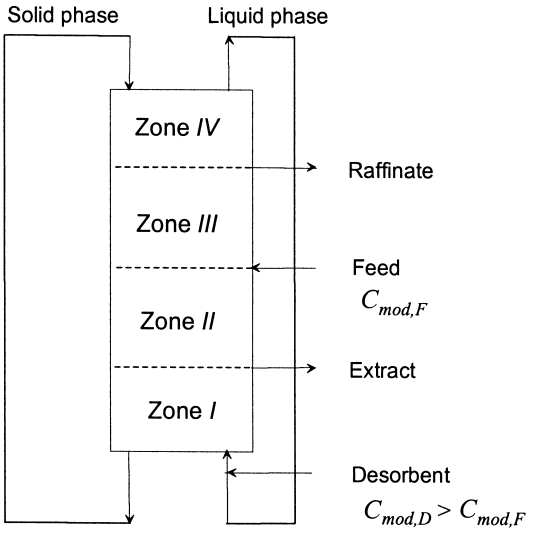

Fig. 1. Scheme of a four-zone two-step gradient TMB process.

2. Two-step gradient SMB technology

The well-known general concept of a classical four-zone TMB process is illustrated schematically in Fig. 1. There are two incoming streams: the feed mixture to be separated and the desorbent or eluent. Two streams leave the unit, one enriched with the less-adsorbable component (raffinate) and one enriched with the more-adsorbable component (extract). The corresponding volumetric flow-rates are $\dot{V}_F$, $\dot{V}_D$, $\dot{V}_R$ and $\dot{V}_E$. These four streams divide the unit into four zones (I, . . . ,IV). Each of the zones has to fulfill distinct tasks [1,11,12].

In implementing the TMB concept using the conventional SMB process, each zone has to contain at least one column. Then by either fixing these columns and shifting the in- and outlet positions co-currently with the fluid flow (moving port implementation) or fixing the in- and outlets and moving the columns counter-currently against the fluid flow (moving column implementation), a counter-current between the two phases is simulated.

The separation of a less-retained component 1 and a more-retained component 2 occurs in the two central zones II and III. Here, the net flow-rates must be set in such a way that component 2 is carried in the direction of the extract outlet and component 1 in the direction of the raffinate outlet. The desorbent is fed to zone I in order to desorb component 2 and thus to regenerate the solid phase. Component 1 is adsorbed on the fresh solid phase in zone IV in order to regenerate the desorbent.

In the conventional isocratic process the solvent strength is identical in all columns (and zones). The simple idea behind the two-step gradient mode is to set the solvent strength in the feed stream lower than that in the desorbent stream. This can be realized, for example, by using in these two inlet streams different concentrations of a stronger solvent (usually called modifier, mod) in a mixture with a weaker solvent. This means, more precisely, that the feed is dissolved in a stream with a lower concentration of the modifier compared to the concentration of the modifier in the desorbent stream ($C_{\mathrm{mod,D}} > C_{\mathrm{mod,F}}$). It is a main result of this approach that the described functions of both regeneration zones I and IV are fulfilled more efficiently. Obviously, this offers the potential to reduce the total solvent amount and hence to increase product concentrations.

3. TMB model

There are several models available to simulate a TMB (see, e.g., Ref. [1]). The most simple model is probably an equilibrium stage model. Using the notation defined in Figs. 2 and 3, in a certain stage X under steady-state conditions the following mass balance holds for the two components that should be separated:

$$\dot{V}_s(C_{S,i,X-1} - C_{S,i,X}) + \dot{V}^{K(X+1)}C_{i,X+1} - \dot{V}^{K(X)}C_{i,X} = -\dot{V}_{ext}C_{i,ext} \quad (1)$$

for $i=1$ or 2 (components of the binary feed mixture), $X = 1,2, \ldots, N^{I} + N^{II} + N^{III} + N^{IV} + 4$ (stages), and $K=$I, II, III or IV (zones), with

$$\dot{V}_{ext}C_{i,ext} = \begin{cases} \dot{V}_F C_{i,F} & \text{feed stage} \\ -\dot{V}_R C_{i,R} & \text{raffinate stage} \\ -\dot{V}_E C_{i,E} & \text{extract stage} \\ 0 & \text{all other stages} \end{cases}$$

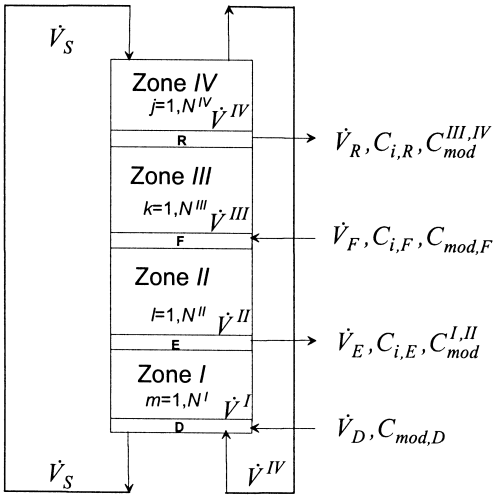

Fig. 2. Description of the cell model used to simulate the two-step gradient TMB process.

where $\dot{V}_s$ is the solid-phase flow-rate, $\dot{V}^K$ the liquid-phase flow-rates in the four zones, C the liquid phase concentrations and C_S the loadings. Different numbers of stages can be assumed in the four zones (N^{I}, N^{II}, N^{III}, N^{IV}), offering the possibility to analyze different zone lengths. These stage numbers can be considered to be lumped parameters taking into account all kinetic effects causing band broadening in a certain zone. As indicated in Fig. 2 there are four distinct stages where the inlet and outlet streams are balanced (D, E, F, R). It is assumed that the desorbent stream is free of component *i*.

In this work the simplifying assumption will be used that, for component *i*, $C_{S,i}$ always depend linearly on the corresponding C_i, i.e.:

$$C_{S,i} = H_i C_i \tag{2}$$

In addition to the balances for components *i* and *j*, the following overall balances at the four specific characteristic stages D, E, F and R also need to be respected (Fig. 2):

$$\dot{V}^{\mathrm{I}} = \dot{V}^{\mathrm{IV}} + \dot{V}_{\mathrm{D}} \tag{3}$$

$$\dot{V}^{\mathrm{II}} = \dot{V}^{\mathrm{I}} - \dot{V}_{\mathrm{E}} \tag{4}$$

$$\dot{V}^{\mathrm{III}} = \dot{V}^{\mathrm{II}} + \dot{V}_{\mathrm{F}} \tag{5}$$

$$\dot{V}^{\mathrm{IV}} = \dot{V}^{\mathrm{III}} - \dot{V}_{\mathrm{R}} \tag{6}$$

An understanding of the closed-loop gradient process under consideration further requires us to follow the local solvent composition, which can be expressed by the concentration of the modifier, C_{mod}. If it is assumed that the modifier is not adsorbable, only the two input stages (D) and (F) need to be analyzed more closely. For them the following balances hold:

$$\dot{V}_{\mathrm{D}} C_{\mathrm{mod,D}} + \dot{V}^{\mathrm{IV}} C^{\mathrm{III,IV}}_{\mathrm{mod}} = \dot{V}^{\mathrm{I}} C^{\mathrm{I,II}}_{\mathrm{mod}} \tag{7}$$

$$\dot{V}_{\mathrm{F}} C_{\mathrm{mod,F}} + \dot{V}^{\mathrm{II}} C^{\mathrm{I,II}}_{\mathrm{mod}} = \dot{V}^{\mathrm{III}} C^{\mathrm{III,IV}}_{\mathrm{mod}} \tag{8}$$

Once all flow-rates and the modifier concentrations in the two inlet streams are specified, the two internal levels of the modifier concentrations in zones I and II (and thus in the extract) and in zones III and IV (and thus in the raffinate) can be determined from Eqs. (7) and (8):

$$C^{\mathrm{I,II}}_{\mathrm{mod}} = (\dot{V}_{\mathrm{F}}\dot{V}^{\mathrm{IV}} C_{\mathrm{mod,F}} + \dot{V}_{\mathrm{D}}\dot{V}^{\mathrm{III}} C_{\mathrm{mod,D}})/ (\dot{V}^{\mathrm{I}}\dot{V}^{\mathrm{III}} - \dot{V}^{\mathrm{II}}\dot{V}^{\mathrm{IV}}) \tag{9}$$

$$C^{\mathrm{III,IV}}_{\mathrm{mod}} = (\dot{V}_{\mathrm{F}}\dot{V}^{\mathrm{I}} C_{\mathrm{mod,F}} + \dot{V}_{\mathrm{D}}\dot{V}^{\mathrm{II}} C_{\mathrm{mod,D}})/ (\dot{V}^{\mathrm{I}}\dot{V}^{\mathrm{III}} - \dot{V}^{\mathrm{II}}\dot{V}^{\mathrm{IV}}) \tag{10}$$

The specification of lower modifier concentrations in the feed than in the desorbent leads to the following relations:

$$C_{\mathrm{mod,D}} > C^{\mathrm{I,II}}_{\mathrm{mod}} > C^{\mathrm{III,IV}}_{\mathrm{mod}} > C_{\mathrm{mod,F}}$$

The effect of the gradient process originates basically from the fact that the local modifier concentrations have an influence on the Henry constants defined in Eq. (2). Usually, this dependence is complex and nonlinear. In this work the following simple relationship, suitable for describing the behavior of normal-phase systems, was used [13]:

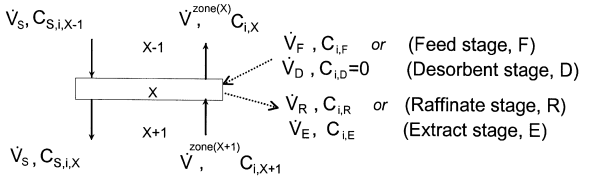

Fig. 3. Schematic representation of an equilibrium stage *X*.

$$H_i(C_{\mathrm{mod}}) = (a_i \cdot C_{\mathrm{mod}})^{-b_i} \quad (11)$$

Due to the considerable numbers of stages that are typical for chromatographic separation processes the system of Eqs. (1)–(11) is usually rather large. To simplify the solution an efficient algorithm was developed exploiting the structure of this system of equations. The essential part consists of using recursion techniques to calculate the coupled balance equations within the four individual zones. Mathematical details will be presented elsewhere [14].

The above set of equations is proposed as a simple model for studying the continuous two-step gradient TMB process and thus also the corresponding SMB process. Due to the possibility of quickly solving the model equations it can be used efficiently in systematic studies screening larger parameter regions. In order to restrict a priori the size of the potential parameter space the analytical solutions offered by equilibrium theory are most instructive.

4. Analysis of linear TMB processes using equilibrium theory

The determination of applicable flow-rates of mobile and solid phases is the most crucial problem in designing TMB and SMB processes. A simple but powerful method to estimate appropriate net flow-rates has been developed for the conventional isocratic process within the framework of equilibrium theory [1,11,12,15]. The concepts neglects all kinetic effects related to mass transfer and finite adsorption and desorption rates. The most essential parameters of the well-established theory are the flow-rate ratios in the four zones, m^K, defined as follows:

$$m^K = \frac{\dot{V}^K}{\dot{V}_S} \quad K = \mathrm{I}, \ldots, \mathrm{IV} \quad (12)$$

In Eq. (12), $\dot{V}_s$ is again the solid-phase flow-rate and $\dot{V}^K$ is the liquid-phase flow-rate in zone K.

The equilibrium theory allows us to specify limits of the flow-rate ratios m^K that need to be fulfilled for a successful operation in the case of infinite efficiency. Under linear and isocratic conditions the following inequalities define a region where a binary feed mixture is completely resolved [11,12]:

$$H_2 < m^{\mathrm{I}} \quad (13)$$

$$H_1 < m^{\mathrm{II}} < m^{\mathrm{III}} < H_2 \quad (14)$$

$$m^{\mathrm{IV}} < H_1 \quad (15)$$

In these equations, H_1 and H_2 are the Henry constants for components 1 and 2, with component 2 being the better-adsorbed ($H_2 > H_1$).

According to the overall mass balances (Eqs. (3)–(6)) the following conditions clearly have to be respected:

$$m^{\mathrm{I}} = m^{\mathrm{IV}} + \frac{\dot{V}_{\mathrm{D}}}{\dot{V}_{\mathrm{S}}} \quad (16)$$

$$m^{\mathrm{II}} = m^{\mathrm{I}} - \frac{\dot{V}_{\mathrm{E}}}{\dot{V}_{\mathrm{S}}} \quad (17)$$

$$m^{\mathrm{III}} = m^{\mathrm{II}} + \frac{\dot{V}_{\mathrm{F}}}{\dot{V}_{\mathrm{S}}} \quad (18)$$

$$m^{\mathrm{IV}} = m^{\mathrm{III}} - \frac{\dot{V}_{\mathrm{R}}}{\dot{V}_{\mathrm{S}}} \quad (19)$$

Specification of the corresponding limits for the flow-rate ratios is more complex in the case of the described two-step gradient mode. Here, the solvent strength in the desorbent stream is set higher than that in the feed stream. This leads to different modifier concentrations in zones I, II and in zones III, IV (with $C_{\mathrm{mod}}^{\mathrm{I,II}} > C_{\mathrm{mod}}^{\mathrm{III,IV}}$) and, consequently, to the following relations for the Henry constants:

$$H_1^{\mathrm{I,II}}(C_{\mathrm{mod}}^{\mathrm{I,II}}) < H_1^{\mathrm{III,IV}}(C_{\mathrm{mod}}^{\mathrm{III,IV}}) \quad (20)$$

$$H_2^{\mathrm{I,II}}(C_{\mathrm{mod}}^{\mathrm{I,II}}) < H_2^{\mathrm{III,IV}}(C_{\mathrm{mod}}^{\mathrm{III,IV}}) \quad (21)$$

Necessary conditions for complete separations for the gradient mode can now be given by the following constraints [5]:

$$H_2^{\mathrm{I,II}}(C_{\mathrm{mod}}^{\mathrm{I,II}}) < m^{\mathrm{I}} \quad (22)$$

$$H_1^{\mathrm{I,II}}(C_{\mathrm{mod}}^{\mathrm{I,II}}) < m^{\mathrm{II}} < H_2^{\mathrm{I,II}}(C_{\mathrm{mod}}^{\mathrm{I,II}}) \quad (23)$$

$$H_1^{\mathrm{III,IV}}(C_{\mathrm{mod}}^{\mathrm{III,IV}}) < m^{\mathrm{III}} < H_2^{\mathrm{III,IV}}(C_{\mathrm{mod}}^{\mathrm{III,IV}}) \quad (24)$$

$$m^{\mathrm{IV}} < H_1^{\mathrm{III,IV}}(C_{\mathrm{mod}}^{\mathrm{III,IV}}) \quad (25)$$

Assuming the case that the two internal modifier concentrations or the corresponding Henry constants could be set fully flexible (not depending on the flow-rates), according to Eqs. (23) and (24) the shape of the separation region would be a truncated rectangle for $H_2^{II} > H_1^{III}$ or a full rectangle for $H_2^{II} < H_1^{III}$ [5]. This flexibility does not exist for the closed-loop arrangement using a liquid mobile phase as discussed here, and more complex shapes of the region result, as will be shown below.

In this work, not only the analysis of the case of infinite efficiencies and complete resolution was intended. To identify suitable operating parameters for more general conditions, only numerical methods could be used. The screening strategies applied in this work and presented below exploit the proposed equilibrium stage model (Eqs. (1)–(11)). However, before analyzing the two-step gradient process in more detail, the general concept of the identification process is discussed for the isocratic process.

5. Identification of suitable operating conditions: isocratic mode

It is well known that the most critical parameters for a successful operation are the flow-rate ratios in separation zones II and III, i.e. m^{II} and m^{III}. To identify suitable parameter constellations, a systematic screening in the (m^{II}, m^{III}) plane was performed. Concerning the determination of the other free parameters required to specify completely a concrete operating point, the strategy suggested in Refs. [11,12] was used.

(1) The performance of the process depends essentially on all four dimensionless flow-rate ratios, m^K. Specification of these values is sufficient for defining a certain process condition on a dimensionless scale. To calculate the corresponding flow-rates $\dot{V}_F$, $\dot{V}_R$, $\dot{V}_E$ and $\dot{V}_D$ explicitly the solid-phase flow-rate $\dot{V}_S$ can be set as a ''scaling'' factor (depending on constraints related to the concrete unit, e.g. pressure drop limitations).

(2) Provided the solid-phase flow-rate $\dot{V}_S$ is specified, for each concrete operating point (m^{II}, m^{III}) the corresponding feed flow-rate, $\dot{V}_F$, can be determined directly from Eq. (18):

$$\frac{\dot{V}_F}{\dot{V}_S} = m^{III} - m^{II} \tag{26}$$

Appropriate values for the remaining two flow-rate ratios m^I and m^{IV} now need to be specified. Since in the two-step gradient mode the modifier mass balances (Eqs. (7) and (8)) need to be respected, this step (3) becomes more complicated. Before analyzing this situation in Section 6 the simpler isocratic case is discussed.

(3) The two required flow-rate ratios m^I and m^{IV} can be determined using a transformation of the inequalities (13) and (15) into equalities by introducing two safety factors, β^I and β^{IV} (both >1). These factors should take the finite efficiencies of the columns into account:

$$m^I = \beta^I H_2 \tag{27}$$

$$m^{IV} = \frac{H_1}{\beta^{IV}} \tag{28}$$

The three remaining external flow-rates can now be calculated from the balance Eqs. (16)–(19):

$$\frac{\dot{V}_E}{\dot{V}_S} = m^I - m^{II} \tag{29}$$

$$\frac{\dot{V}_R}{\dot{V}_S} = m^{III} - m^{IV} \tag{30}$$

$$\frac{\dot{V}_D}{\dot{V}_S} = m^I - m^{IV} \tag{31}$$

It should be noted that, using this well-known approach for the isocratic process, the desorbent flow-rate, $\dot{V}_D$, is constant for all pairs (m^{II}, m^{III}) and does not depend on variations of the feed flow-rate, $\dot{V}_F$. With respect to minimizing the desorbent flow-rate the optimal safety factors are obviously $\beta^I = \beta^{IV} = 1$.

To evaluate the process performance and to identify regions of suitable operating conditions, a sufficiently large plane of (m^{II}, m^{III}) values can be inspected systematically within the screening process. For each analyzed operation point the purities at the two outlets can be evaluated:

$$Pu_{i,\mathrm{port}} = 100\% \cdot \frac{C_{i,\mathrm{port}}}{C_{1,\mathrm{port}} + C_{2,\mathrm{port}}}$$
$$i = 1,2; \quad \mathrm{port} = \mathrm{E,R} \tag{32}$$

In this way, (m^{II}, m^{III}) regions allowing us to reach certain specified purities (not necessarily 100%) can be marked. The location and shape of these regions is affected strongly by the Henry constants of the components to be separated and also by the column efficiencies (i.e. the numbers of stages in the four zones), the chosen safety factors $\beta^{\mathrm{I}}$and β^{IV} and the specified purity requirements.

Figs. 4 and 5 show typical results of a systematic screening for the isocratic process and the two Henry constants $H_1 = 5$ and $H_2 = 10$.

Region A in Fig. 4 shows the available parameter range in the (m^{II}, m^{III}) plane for a very efficient system ($N^{\mathrm{total}} = 40\,004$) and very high purities ($Pu_{1,\mathrm{R}} = Pu_{2,\mathrm{E}} > 99.99\%$). The obtained numerical results confirm completely the results of the equilibrium theory predicting that the region is triangular and fixed at the values of the two Henry constants (Eq. (14)). Compared to this ideal situation, a decrease of the system efficiency leads to the expected shrinking of the separation region ($N^{\mathrm{total}} = 404$, region B), even if both safety factors, β^{I} and β^{IV}, are increased from 1.001 to 1.1. Decreasing the purity requirements from 99.99 to 95% (region C) naturally leads to an increase of the region size (more operating parameters are available to fulfill the task and, in particular, more feed can be processed).

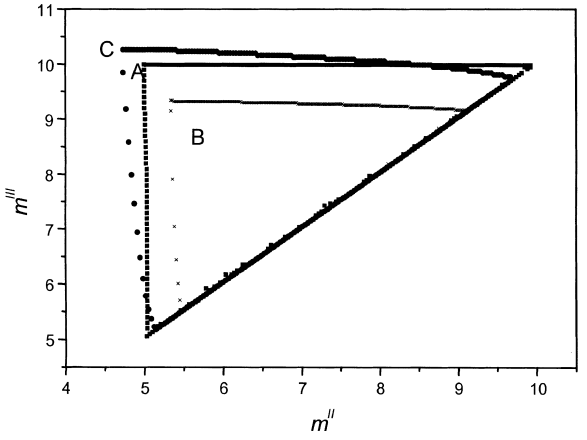

Fig. 4. Separation regions for the isocratic mode, $H_1 = 5$, $H_2 = 10$. Region A: $N^{\mathrm{I}} = N^{\mathrm{II}} = N^{\mathrm{III}} = N^{\mathrm{IV}} = 10\,000$, $Pu_{1,\mathrm{R}} > 99.99\%$, $Pu_{2,\mathrm{E}} > 99.99\%$, $\beta^{\mathrm{I}} = \beta^{\mathrm{IV}} = 1.001$. Region B: $N^{\mathrm{I}} = N^{\mathrm{II}} = N^{\mathrm{III}} = N^{\mathrm{IV}} = 100$, $Pu_{1,\mathrm{R\ E}} > 99.99\%$, $Pu_{2,\mathrm{E}} > 99.99\%$, $\beta^{\mathrm{I}} = \beta^{\mathrm{IV}} = 1.1$. Region C: $N^{\mathrm{I}} = N^{\mathrm{II}} = N^{\mathrm{III}} = N^{\mathrm{IV}} = 100$, $Pu_{1,\mathrm{R}} > 95\%$, $Pu_{2,\mathrm{E}} > 95\%$, $\beta^{\mathrm{I}} = \beta^{\mathrm{IV}} = 1.1$.

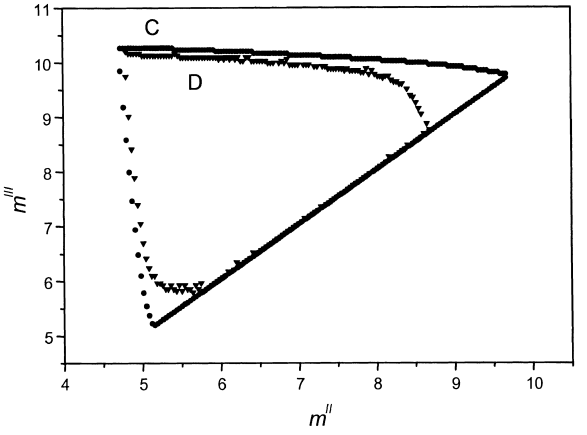

Fig. 5. Separation regions for the isocratic mode, $H_1 = 5$, $H_2 = 10$. $N^{\mathrm{I}} = N^{\mathrm{II}} = N^{\mathrm{III}} = N^{\mathrm{IV}} = 100$, $Pu_{1,\mathrm{R}} > 95\%$, $Pu_{2,\mathrm{E}} > 95\%$. Region C: $\beta^{\mathrm{I}} = \beta^{\mathrm{IV}} = 1.1$ (the same as region C in Fig. 4). Region D: $\beta^{\mathrm{I}} = \beta^{\mathrm{IV}} = 1.001$.

In Fig. 5 (region D) a case is illustrated where, for lower efficiencies, the safety factors $\beta^{\mathrm{I}}$and β^{IV} are too small to always ensure a sufficient regeneration of the solid and liquid phases ($\beta^{\mathrm{I}} = \beta^{\mathrm{IV}} = 1.001$ instead of 1.1 for region C). Malfunction of the regeneration regions reduces the size of the applicable parameter space. However, the separation can still be performed in the most interesting parameter range in which the difference $m^{\mathrm{III}} - m^{\mathrm{II}}$ is maximal, i.e. where most feed can be processed (Eq. (26)).

Below, results will be presented mainly where the number of equilibrium stages was set to be $N^{\mathrm{total}} = 404$ ($4 \cdot 100 + 4$) and where reduced purity requirements of $Pu_{1,\mathrm{R}} = Pu_{2,\mathrm{E}} > 95$ were considered. Results of further studies (not presented here) revealed that the general tendencies and conclusions that will be presented do not depend on this choice.

6. Screening strategies for the gradient mode

After discussing the isocratic process we will now come back to the two-step gradient process. Since the first two steps for the determination of regions of

complete separation described above are identical we will immediately turn to step 3 where now the two different concentrations of the modifier in the feed and desorbent stream, $C_{\mathrm{mod,D}}$ and $C_{\mathrm{mod,F}}$, have to be taken into account. The required specification of these two parameters offers different options to formulate constraints during screening in the (m^{II}, m^{III}) plane. In general, these options lead to different implicit mathematical formulations of the problem and to different sizes and shapes of the separation regions, as will be shown below for two different possibilities (denoted as strategies 3A and 3B). In any case, for each (m^{II}, m^{III}) pair the two levels of the internal modifier concentrations $C^{\mathrm{I,II}}_{\mathrm{mod}}$ and $C^{\mathrm{III,IV}}_{\mathrm{mod}}$ have to be calculated. These values deliver the information required to specify the local Henry constants. However, they also influence the values for the remaining flow-rate ratios m^{I} and m^{IV}. After discussing the two options 3A and 3B based on solving the implicit formulation of the problem, two approaches rendering the problem explicit will be discussed (strategies 3C and 3D).

6.1. Implicit formulations

6.1.1. Strategy 3A (setting $C_{mod,D}$, $C_{mod,F}$, β^I and β^{IV})

Expressing the modifier mass balance Eqs. (9) and (10) as a function of the dimensionless flow-rate ratios and specifying m^{I} and m^{IV} using the two safety factors $\beta^{\mathrm{I}}$and β^{IV}(Eqs. (27) and (28)) leads to:

$$0 = C^{\mathrm{I,II}}_{\mathrm{mod}} - \frac{[H_1(C^{\mathrm{III,IV}}_{\mathrm{mod}})/\beta^{\mathrm{IV}}]\cdot(m^{\mathrm{III}}-m^{\mathrm{II}})C_{\mathrm{mod,F}}+m^{\mathrm{III}}\{\beta^{\mathrm{I}}H_2(C^{\mathrm{I,II}}_{\mathrm{mod}})-[H_1(C^{\mathrm{III,IV}}_{\mathrm{mod}})/\beta^{\mathrm{IV}}]\}C_{\mathrm{mod,D}}}{\beta^{\mathrm{I}}H_2(C^{\mathrm{I,II}}_{\mathrm{mod}})m^{\mathrm{III}}-[H_1(C^{\mathrm{III,IV}}_{\mathrm{mod}})/\beta^{\mathrm{IV}}]m^{\mathrm{II}}} \tag{33}$$

$$0 = C^{\mathrm{III,IV}}_{\mathrm{mod}} - \frac{\beta^{\mathrm{I}}H_2(C^{\mathrm{I,II}}_{\mathrm{mod}})(m^{\mathrm{III}}-m^{\mathrm{II}})C_{\mathrm{mod,F}}+m^{\mathrm{II}}\{\beta^{\mathrm{I}}H_2(C^{\mathrm{I,II}}_{\mathrm{mod}})-[H_1(C^{\mathrm{III,IV}}_{\mathrm{mod}})/\beta^{\mathrm{IV}}]\}C_{\mathrm{mod,D}}}{\beta^{\mathrm{I}}H_2(C^{\mathrm{I,II}}_{\mathrm{mod}})m^{\mathrm{III}}-[H_1(C^{\mathrm{III,IV}}_{\mathrm{mod}})/\beta^{\mathrm{IV}}]m^{\mathrm{II}}} \tag{34}$$

Once the dependence of the Henry constants on the modifier concentration is fixed, from Eqs. (33) and (34) $C^{\mathrm{I,II}}_{\mathrm{mod}}$ and $C^{\mathrm{III,IV}}_{\mathrm{mod}}$ can be calculated using standard nonlinear equation solvers (e.g., the Newton–Raphson method). Subsequently, all the other unknown parameters belonging to a certain operation point follow in a straightforward manner.

For the concrete functional dependence of the Henry constants on the modifier concentrations chosen in this work (Eq. (11)) the nonlinear problem that needs to be solved becomes:

$$0 = C^{\mathrm{I,II}}_{\mathrm{mod}} - \frac{[1/\beta^{\mathrm{IV}}(a_1C^{\mathrm{III,IV}}_{\mathrm{mod}})^{b_1}](m^{\mathrm{III}}-m^{\mathrm{II}})C_{\mathrm{mod,F}}+m^{\mathrm{III}}\{[\beta^{\mathrm{I}}/(a_2C^{\mathrm{I,II}}_{\mathrm{mod}})^{b_2}]-[1/\beta^{\mathrm{IV}}(a_1C^{\mathrm{III,IV}}_{\mathrm{mod}})^{b_1}]\}C_{\mathrm{mod,D}}}{[\beta^{\mathrm{I}}/(a_2C^{\mathrm{I,II}}_{\mathrm{mod}})^{b_2}]m^{\mathrm{III}}-m^{\mathrm{II}}[1/\beta^{\mathrm{IV}}(a_1C^{\mathrm{III,IV}}_{\mathrm{mod}})^{b_1}]} \tag{35}$$

$$0 = C^{\mathrm{III,IV}}_{\mathrm{mod}} - \frac{[\beta^{\mathrm{I}}/(a_2C^{\mathrm{I,II}}_{\mathrm{mod}})^{b_2}](m^{\mathrm{III}}-m^{\mathrm{II}})C_{\mathrm{mod,F}}+m^{\mathrm{II}}\{[\beta^{\mathrm{I}}/(a_2C^{\mathrm{I,II}}_{\mathrm{mod}})^{b_2}]-[1/\beta^{\mathrm{IV}}(a_1C^{\mathrm{III,IV}}_{\mathrm{mod}})^{b_1}]\}C_{\mathrm{mod,D}}}{[\beta^{\mathrm{I}}/(a_2C^{\mathrm{I,II}}_{\mathrm{mod}})^{b_2}]m^{\mathrm{III}}-m^{\mathrm{II}}[1/\beta^{\mathrm{IV}}(a_1C^{\mathrm{III,IV}}_{\mathrm{mod}})^{b_1}]} \tag{36}$$

6.1.2. Strategy 3B (setting $C_{mod,F}$, an averaged modifier concentration $\bar{C}_{mod}$, β^I and β^{IV})

Instead of setting both input modifier concentrations, an alternative way is based on fixing an average value of the modifier concentration in the unit. Such an averaged modifier concentration can be defined as follows:

$$\bar{C}_{\mathrm{mod}} = \frac{\dot{V}_{\mathrm{F}}C_{\mathrm{mod,F}} + \dot{V}_{\mathrm{D}}C_{\mathrm{mod,D}}}{\dot{V}_{\mathrm{F}} + \dot{V}_{\mathrm{D}}} \tag{37}$$

If this averaged modifier concentration and the modifier concentration in the feed are specified, for the modifier concentration at the desorbent port holds:

$$C_{\mathrm{mod,D}} = \frac{\dot{V}_{\mathrm{F}} + \dot{V}_{\mathrm{D}}}{\dot{V}_{\mathrm{D}}}\cdot\bar{C}_{\mathrm{mod}} - \frac{\dot{V}_{\mathrm{F}}}{\dot{V}_{\mathrm{D}}}\cdot C_{\mathrm{mod,F}} \tag{38}$$

This quantity can also be expressed as a function of the parameters m^{II}, m^{III}, β^{I} and $\beta^{\mathrm{IV}}$and the isotherm parameters:

$$C_{\mathrm{mod,D}} = \left(\frac{(m^{\mathrm{III}}-m^{\mathrm{II}})}{[\beta^{\mathrm{I}}/(a_2C^{\mathrm{I,II}}_{\mathrm{mod}})^{b_2}]-[1/\beta^{\mathrm{IV}}(a_1C^{\mathrm{III,IV}}_{\mathrm{mod}})^{b_1}]}+1\right)\cdot\bar{C}_{\mathrm{mod}} - \frac{m^{\mathrm{III}}-m^{\mathrm{II}}}{[\beta^{\mathrm{I}}/(a_2C^{\mathrm{I,II}}_{\mathrm{mod}})^{b_2}]-[1/\beta^{\mathrm{IV}}(a_1C^{\mathrm{III,IV}}_{\mathrm{mod}})^{b_1}]}\cdot C_{\mathrm{mod,F}} \tag{39}$$

Substituting Eq. (39) into Eqs. (35) and (36) leads to the problem of situation 3A and again the solution of the two nonlinear equations gives $C_{\mathrm{mod}}^{\mathrm{I,II}}$ and $C_{\mathrm{mod}}^{\mathrm{III,IV}}$ and hence all the other unknown parameter including the actual modifier concentration in the desorbent stream, $C_{\mathrm{mod,D}}$. Obviously, only values fulfilling $C_{\mathrm{mod,D}} \leq 100\%$ are physically significant.

6.1.3. Isotherm parameters

For the calculations presented below a concrete dependence of the isotherm parameters on the modifier concentration according to Eq. (11) was chosen. The following parameters were used: $a_1 = 0.02$, $a_2 = 0.01$, $b_1 = b_2 = 1$. These parameters lead to $H_1 = 50/C_{\mathrm{mod}}$ and $H_2 = 100/C_{\mathrm{mod}}$. Thus, independent of the modifier concentration, a constant selectivity factor of 2 was assumed. The corresponding dependence of the two Henry constants on the modifier concentration is shown in Fig. 6. For $C_{\mathrm{mod}} = 10\%$ these constants are $H_1 = 5$ and $H_2 = 10$, as assumed before in the study of the isocratic case (Figs. 4 and 5).

6.1.4. Results for strategy 3A (setting $C_{mod,D}$, $C_{mod,F}$, β^I and β^{IV})

In several series of calculations the (m^{II}, m^{III}) plane was screened systematically to identify suitable separation regions. Besides setting $N^{\mathrm{I}} = N^{\mathrm{II}} = N^{\mathrm{III}} = N^{\mathrm{IV}} = 100$ and $Pu_{1,\mathrm{R}} = Pu_{2,\mathrm{E}} = 95\%$, the safety factors were assumed to be $\beta^{\mathrm{I}} = \beta^{\mathrm{IV}} = 1.1$.

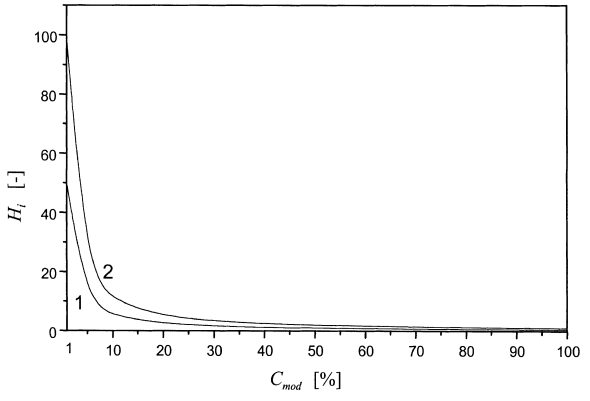

Fig. 6. Plot of the dependence of the two Henry constants H_1 and H_2 on the modifier concentration according to Eq. (11) with the following parameters: $a_1 = 0.02$, $a_2 = 0.01$, $b_1 = b_2 = 1$, i.e. $H_1 = 50/C_{\mathrm{mod}}$ and $H_2 = 100/C_{\mathrm{mod}}$.

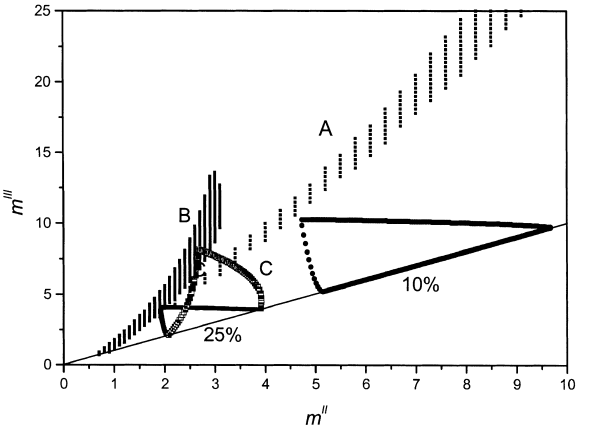

Fig. 7. Separation regions for strategy 3A (implicit formulation). $N^{\mathrm{I}} = N^{\mathrm{II}} = N^{\mathrm{III}} = N^{\mathrm{IV}} = 100$, $Pu_{1,\mathrm{R}} \geq 95\%$, $Pu_{2,\mathrm{E}} > 95\%$, $\beta^{\mathrm{I}} = \beta^{\mathrm{IV}} = 1.1$. 10%: isocratic cases: $\bar{C}_{\mathrm{mod}}^{\mathrm{iso}} = 10\%$. 25%: isocratic cases: $\bar{C}_{\mathrm{mod}}^{\mathrm{iso}} = 25\%$. Region A: $C_{\mathrm{mod,F}} = 1\%$, $C_{\mathrm{mod,D}} = 100\%$ (only partly depicted; fully in Fig. 15). Region B: $C_{\mathrm{mod,F}} = 5\%$, $C_{\mathrm{mod,D}} = 100\%$. Region C: $C_{\mathrm{mod,F}} = 10\%$, $C_{\mathrm{mod,D}} = 25\%$.

Typical separation regions for various concentrations of the modifier in the feed and desorbent streams, $C_{\mathrm{mod,F}}$ and $C_{\mathrm{mod,D}}$, are shown in Fig. 7. For comparison, at first two isocratic situations have been analyzed for 10 and 25% modifier concentrations. As expected, an increase of this concentration related to a decrease of the Henry constants shifts the separation regions in the (m^{II}, m^{II}) plane towards the origin. Selected results for three gradient situations using strategy 3A (regions A, B and C) reveal that, in this case, the shape and location of the region is clearly rather complex. Apparently, the larger the difference between the modifier concentrations in the two feed streams (i.e. the higher the ''driving force'' for the gradient) the higher the feed flow-rates that could be processed (indicated by the increasing accessible maximum differences between m^{III} and m^{II} for regions C→B→A). In parallel, the regions change their shape more and more compared to the isocratic case. They become narrower and a practical realization for larger gradient driving forces is rendered more difficult. In evaluating strategy 3A it should be kept in mind that, in a certain separation region belonging to the same $C_{\mathrm{mod,F}}$ and $C_{\mathrm{mod,D}}$ values, individual operating points correspond to different ratios between the two inlet flow-rates for feed and desorbent. This leads to different internal

modifier concentrations, $C_{\mathrm{mod}}^{\mathrm{I,II}}$ and $C_{\mathrm{mod}}^{\mathrm{III,IV}}$. Obviously, for relatively low feed flow-rates the internal modifier concentrations are close to that in the desorbent stream, while for relatively high feed flow-rates they are close to that in the feed stream. For region B of Fig. 7 the corresponding regions of the two internal modifier concentrations are shown in Fig. 8 as a function of the distance from the diagonal, i.e. of $\dot{V}_{\mathrm{F}}/\dot{V}_{\mathrm{S}}$ or $m^{\mathrm{III}} - m^{\mathrm{II}}$. Obviously, a desirable increase of the feed flow-rate reduces, in a similar manner, both the local modifier concentrations and thus the averaged modifier concentration in the unit. The resulting difference between the two internal modifier concentrations (i.e. the gradient driving force) is hardly affected by the increase of the feed flow-rate.

6.1.5. Results for strategy 3B (setting $C_{mod,F}$, $\bar{C}_{mod}$, β^{I} and β^{IV})

The a priori fixation of an averaged modifier concentration in the unit, $\bar{C}_{\mathrm{mod}}$, leads to another situation. Now within a separation region, operating points are found corresponding to different modifier concentrations in the desorbent stream. The maintenance of the required averaged modifier concentration causes an additional constraint compared to the previous situation. Now it is not possible to maximize unlimited $\dot{V}_{\mathrm{F}}$ and to keep in parallel $\dot{V}_{\mathrm{D}}$ constant or even to reduce it. Both flow-rates are linked according to Eq. (37):

$$\frac{\dot{V}_{\mathrm{F}}}{\dot{V}_{\mathrm{D}}} = \frac{C_{\mathrm{mod,D}} - \bar{C}_{\mathrm{mod}}}{\bar{C}_{\mathrm{mod}} - C_{\mathrm{mod,F}}} \tag{40}$$

The most attractive ratio is possible for $C_{\mathrm{mod,F}} = 0\%$ and $C_{\mathrm{mod,D}} = 100\%$. If these two inlet modifier concentrations are used the processing of more feed always requires more solvent.

Typical separation regions are given in Fig. 9 for an averaged modifier concentration of 10%. Region A represents the isocratic case already shown in Fig. 7. Regions B, C and D were calculated for three different modifier concentrations in the feed using for each operating point the implicit procedure based on solving Eqs. (35), (36) and (39).

Considering a feed that is free of modifier, $C_{\mathrm{mod,F}} = 0\%$ (region B), there is practically no marked change in the size of the separation region and thus in the productivity of the process compared to the isocratic case. There is, however, a significant reduction in the desorbent consumption, as will be discussed in Section 6.3.

An increase of the modifier concentration in the feed stream to 3 and 5% (regions C and D) leads to separation regions that become longer, and larger feed flow-rates can be used. However, growth of the regions leads to a distinct maximum which coincides for this case approximately with region D. For larger modifier concentrations in the feed (not presented in Fig. 9), the regions become smaller again and

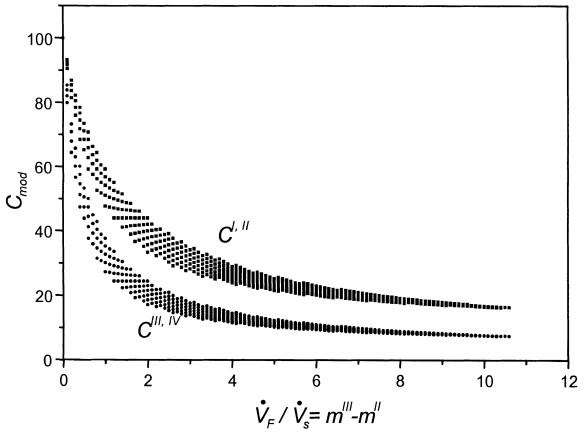

Fig. 8. The regions of the two internal modifier concentrations corresponding to separation region B in Fig. 7 (strategy 3A).

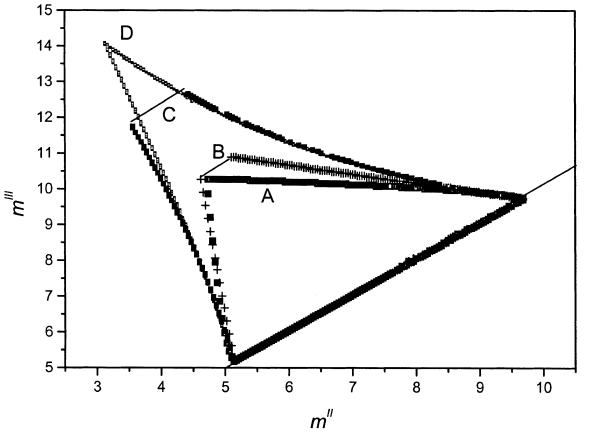

Fig. 9. Separation regions for strategy 3B (implicit formulation). $\bar{C}_{\mathrm{mod}} = 10\%$, $N^{\mathrm{I}} = N^{\mathrm{II}} = N^{\mathrm{III}} = N^{\mathrm{IV}} = 100$, $Pu_{1,\mathrm{R}} > 95\%$, $Pu_{2,\mathrm{E}} > 95\%$, $\beta^{\mathrm{I}} = \beta^{\mathrm{IV}} = 1.1$. Region A: isocratic. Region B: $C_{\mathrm{mod,F}} = 0\%$. Region C: $C_{\mathrm{mod,F}} = 3\%$. Region D: $C_{\mathrm{mod,F}} = 5\%$.

gradually reach the region for the corresponding isocratic situation.

Controlling the averaged modifier concentration in the unit also has an impact on the levels of the two internal modifier concentrations in zones I, II and III, IV. As shown in Fig. 10, and in contrast to strategy 3A (Fig. 8), an increase of the feed flow-rate now leads to an increase of the difference between these internal modifier concentrations. This is again due to the fact that the modifier mass balance requires, for higher feed flow-rates, higher modifier concentrations in the desorbent stream. The maximal difference is always reached for $C_{\mathrm{mod,D}} = 100\%$, corresponding to the maximal feed flow-rate that could be processed.

6.2. Explicit formulations

The results presented above for strategies 3A and 3B were based on calculating iteratively the two internal modifier concentrations. Following strategy 3B and fixing the averaged modifier concentration, $\bar{C}_{\mathrm{mod}}$, two explicit formulations can be derived which will be considered below (strategies 3C and 3D).

6.2.1. Strategy 3C (setting $\bar{C}_{mod}$, $C_{mod,F}$, β^{I}_{3C} and β^{IV}_{3C})

The a_priori specified averaged modifier concentration C_{mod} may be used directly to estimate for each pair (m^{II}, m^{III}) the required Henry constants and the remaining flow-rate ratios. Thus, instead of Eqs. (27) and (28) (adapted to the gradient situation):

$$m^{\mathrm{I}} = H_2(C^{\mathrm{I,II}}_{\mathrm{mod}})\beta^{\mathrm{I}} \tag{41}$$

$$m^{\mathrm{IV}} = H_1(C^{\mathrm{III,IV}}_{\mathrm{mod}})/\beta^{\mathrm{IV}} \tag{42}$$

the following two equations can be used:

$$m^{\mathrm{I}} = H_2(\bar{C}_{\mathrm{mod}})\beta^{\mathrm{I}}_{\mathrm{3C}} \tag{43}$$

$$m^{\mathrm{IV}} = H_1(\bar{C}_{\mathrm{mod}})/\beta^{\mathrm{IV}}_{\mathrm{3C}} \tag{44}$$

The new safety factors $\beta^{\mathrm{I}}_{\mathrm{3C}}$ and $\beta^{\mathrm{IV}}_{\mathrm{3C}}$ introduced in Eqs. (43) and (44) also incorporate the missing knowledge about the two actual internal modifier concentrations. Strategy 3C leads to a constant desorbent flow-rate in the whole separation region and does not impose restrictions concerning the size of the feed flow-rate. A typical separation region for strategy 3C is illustrated as region C in Fig. 11. It is considerably larger compared to the corresponding isocratic mode (region A) and to the region obtained using strategy 3B (region B). Indicated by the accessible differences between m^{III} and m^{II}, higher feed flow-rates can be treated. Obviously, this simple and explicit design strategy can lead to separation

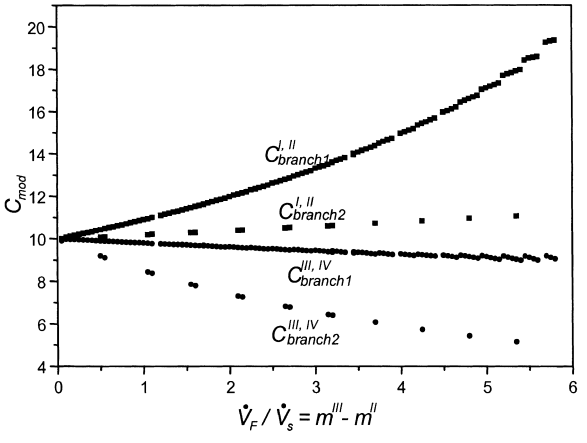

Fig. 10. Borders of the regions of the two internal modifier concentrations corresponding to separation region B in Fig. 9 (strategy 3B).

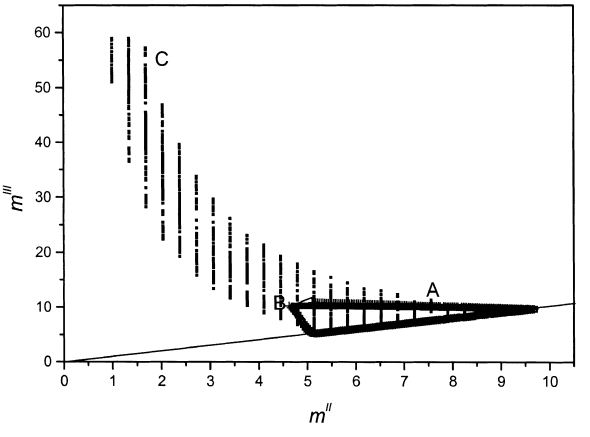

Fig. 11. Separation region (C) for strategy 3C using the explicit formulation with $H(\bar{C}_{\mathrm{iso}})$ and Eqs. (43) and (44). Regions A (isocratic) and B (strategy 3B) as in Fig. 9. $\bar{C}_{\mathrm{mod}} = 10\%$, $C_{\mathrm{mod,F}} = 0\%$, $N^{\mathrm{I}} = N^{\mathrm{II}} = N^{\mathrm{III}} = N^{\mathrm{IV}} = 100$, $Pu_{1,\mathrm{R}} > 95\%$, $Pu_{2,\mathrm{E}} > 95\%$, $\beta^{\mathrm{I}}_{\mathrm{3C}} = \beta^{\mathrm{IV}}_{\mathrm{3C}} = 1.1$.

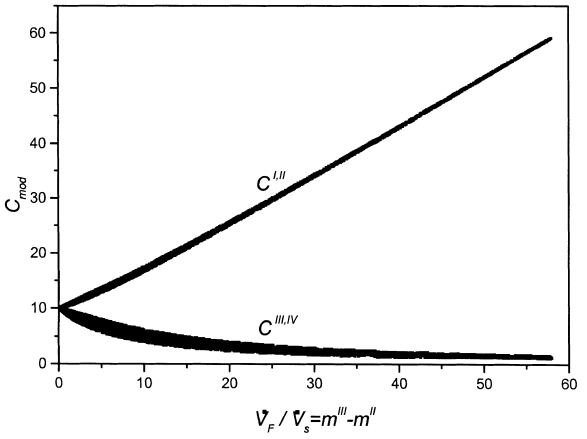

Fig. 12. Borders of the regions of the two internal modifier concentrations corresponding to separation region C in Fig. 11 (strategy 3C).

regions offering the potential for significant improvements.

Fig. 12 shows the corresponding regions of the two internal modifier levels for strategy 3C. As for strategy 3B, increased feed flow-rates create larger differences of these values. The values of these internal modifier concentrations further allow us to calculate safety factors β^{I} and β^{IV} from Eqs. (41) and (42) corresponding to those used in strategies 3A and 3B. Fig. 13 shows that these safety factors increase with increasing feed flow-rates. Rather large values of up to 12 are reached.

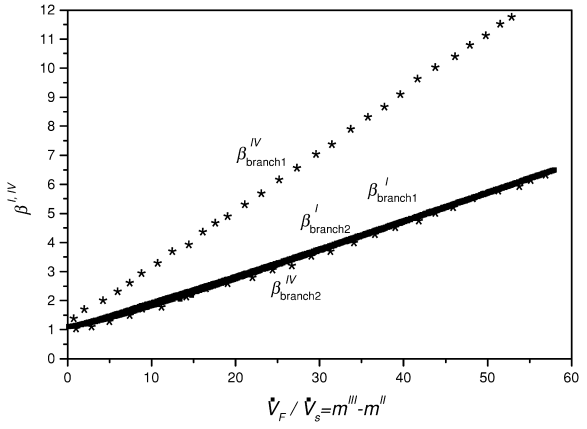

Fig. 13. Changes of the safety factors β^{I} and β^{IV} (Eqs. (41) and (42)) with the feed flow-rate for $\beta^{I}_{3C} = \beta^{IV}_{3C} = 1.1$ (Eqs. (43) and (44)). Corresponds to region C in Fig. 11 (strategy 3C).

6.2.2. Strategy 3D (setting $\bar{C}_{mod}$, $C_{mod,F}$, β^{I}_{3D} and β^{IV}_{3D})

Instead of using Eqs. (43) and (44) there is another simple way to specify for each pair (m^{II}, m^{III}) the remaining two flow-rate ratios m^{I} and m^{IV}. These values can be determined from the differences between two of the four inequalities given with Eqs. (22)–(25) after transforming them into equalities by introducing two other factors, β^{I}_{3D} and β^{IV}_{3D}:

$$m^{I} = m^{II} + \beta^{I}_{3D}(H^{I,II}_{2} - H^{I,II}_{1}) \tag{45}$$

(from the difference between Eqs. (22) and (23)).

$$m^{IV} = m^{III} + (H^{III,IV}_{1} - H^{III,IV}_{2})/\beta^{IV}_{3D} \tag{46}$$

(from the difference between Eqs. (24) and (25))

If, again, the local Henry constants are estimated based on the specified average modifier concentration, the two outlet flow-rates $\dot{V}_E$ and $\dot{V}_R$ can be calculated directly from Eqs. (17), (19), (45) and (46):

$$\frac{\dot{V}_E}{\dot{V}_S} = \beta^{I}_{3D}[H_2(\bar{C}_{mod}) - H_1(\bar{C}_{mod})] \tag{47}$$

$$\frac{\dot{V}_R}{\dot{V}_S} = [H_2(\bar{C}_{mod}) - H_1(\bar{C}_{mod})]/\beta^{IV}_{3D} \tag{48}$$

In strategy 3D, $\dot{V}_E$ and $\dot{V}_R$ are constant for each (m^{II}, m^{III}) pair and $\dot{V}_D$ varies as $\dot{V}_F$. More explicitly, $\dot{V}_D$ decreases if $\dot{V}_F$ is increased, which is obviously a favorable feature of this strategy. Related to this procedure is the fact that the safety factors $\beta^{I}$and β^{IV}corresponding to Eqs. (41) and (42) and used in strategies 3A and 3B vary in the (m^{II}, m^{III}) plane according to:

$$\beta^{I} = \frac{m^{II} + \beta^{I}_{3D}[H_2(\bar{C}_{mod}) - H_1(\bar{C}_{mod})]}{H_2[C^{I,II}_{mod}(m^{I},m^{IV})]} \tag{49}$$

$$\beta^{IV} = \frac{H_1[C^{III,IV}_{mod}(m^{I},m^{IV})]}{m^{III} - [H_2(\bar{C}_{mod}) - H_1(\bar{C}_{mod})]/\beta^{IV}_{3D}} \tag{50}$$

Systematic screening of m^{II} and m^{III} values was first performed using strategy 3D for two levels of the averaged modifier concentrations: $\bar{C}_{mod} = 10$ and

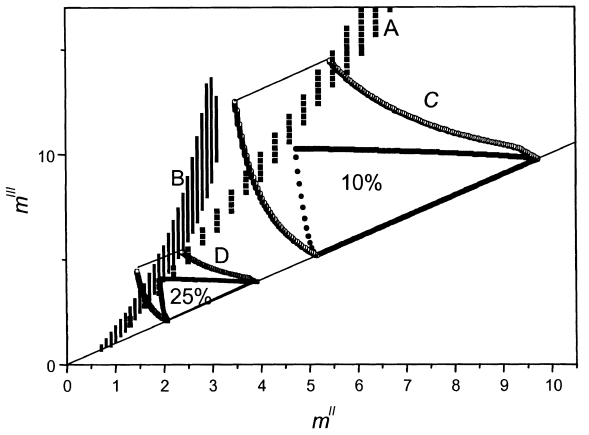

Fig. 14. Separation regions for strategy 3D using the explicit formulation with $H(\bar{C}_{mod})$ and Eqs. (47) and (48). $N^{I} = N^{II} = N^{III} = N^{IV} = 100$, $Pu_{1,R} > 95\%$, $Pu_{2,E} > 95\%$, $\beta^{I}_{3D} = \beta^{IV}_{3D} = 1.1$. Region C: $\bar{C}_{mod} = 10\%$, $C_{mod,F} = 0\%$. Region D: $\bar{C}_{mod} = 25\%$, $C_{mod,F} = 0\%$. Regions 10% and 25% (isocratic) and A, B (strategy 3A): as in Fig. 7.

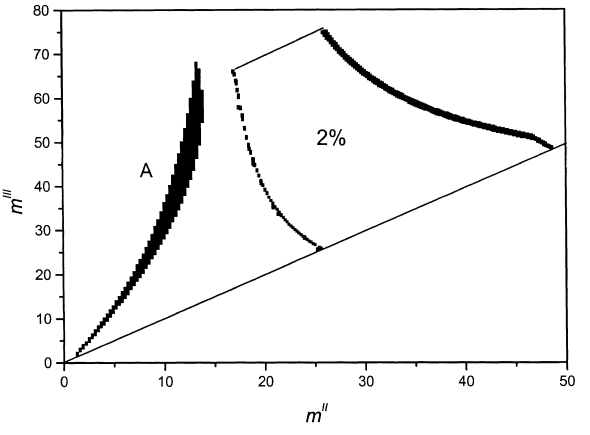

Fig. 15. Separation regions for strategy 3D using the explicit formulation with $H(\bar{C}_{mod})$ and Eqs. (47) and (48). $\bar{C}_{mod} = 2\%$, $C_{mod,F} = 0\%$, $N^{I} = N^{II} = N^{III} = N^{IV} = 100$, $Pu_{1,R} > 95\%$, $Pu_{2,E} > 95\%$, $\beta^{I}_{3D} = \beta^{IV}_{3D} = 1.1$. Region A: as in Fig. 7 (strategy 3A).

25%. The obtained separation regions are depicted in Fig. 14. For comparison, the separation regions for the isocratic case and for strategy 3A are also depicted. The obtained regions C and D are considerably larger than the isocratic regions and allow us to process larger feed flow-rates. The maximal feed flow-rate is related to $C_{mod,D} = 100\%$. Hence, the size of the separation region is bounded in the (m^{II}, m^{III}) plane by a parallel to the diagonal where the same feed amount is treated and pure modifier is used as the desorbent. Compared to regions A and B obtained with strategy 3A, regions C and D obtained with strategy 3D are much wider, and a more robust operation close to the optimal points can be expected. This favorable feature is further exemplified in Fig. 15 where the complete region A (strategy 3A) is shown in contrast to the accessible region determined with strategy 3D for a reduced averaged modifier concentration of $\bar{C}_{mod} = 2\%$.

To study the effect of the factors $\beta^{I}_{3D} = \beta^{IV}_{3D}$ on the shape of the separation regions, further calculations were carried out. Due to their definition, these factors cannot be considered as safety factors related to ensure the fulfillment of a certain zone-dependent task. Thus, values below unity may also be acceptable. To eliminate in these calculations the influence of column efficiencies and reduced purity requirements, $N = 10\,000$ and $Pu > 99.99\%$ were assumed. Three sets of calculations were performed for $\beta^{I}_{3D} = \beta^{IV}_{3D} = 1$, $\beta^{I}_{3D} = \beta^{IV}_{3D} = 1.5$ and $\beta^{I}_{3D} = 1.5/\beta^{IV}_{3D} = 1/1.5$. Fig. 16 shows the separation regions obtained. A detailed analysis of the shape of these regions is outside the scope of this paper. However, the considerable potential of choosing reasonable factors β^{I}_{3D} and β^{IV}_{3D} is obvious.

As shown before for strategies 3B and 3C in Figs.

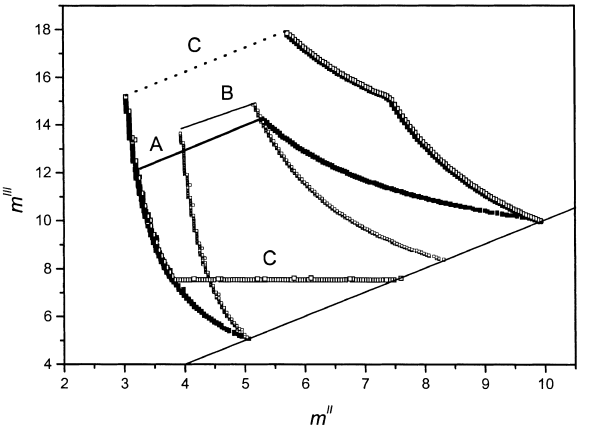

Fig. 16. Separation regions for strategy 3D using the explicit formulation with $H(\bar{C}_{mod})$ and Eqs. (47) and (48). $\bar{C}_{mod} = 10\%$, $C_{mod,F} = 0\%$, $N^{I} = N^{II} = N^{III} = N^{IV} = 10\,000$, $Pu_{1,R} > 99.99\%$, $Pu_{2,E} > 99.99\%$. Region A: $\beta^{I}_{3D} = \beta^{IV}_{3D} = 1$. Region B: $\beta^{I}_{3D} = \beta^{IV}_{3D} = 1.5$. Region C: $\beta^{I}_{3D} = 1.5$ and $\beta^{IV}_{3D} = 1/1.5$.

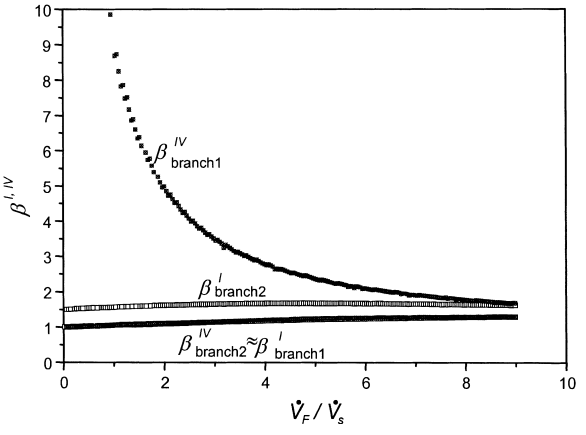

Fig. 17. Changes of the safety factors β^{I} and β^{IV}(Eqs. (41) and (42)) with feed flow-rate corresponding to separation region A in Fig. 16 (strategy 3D).

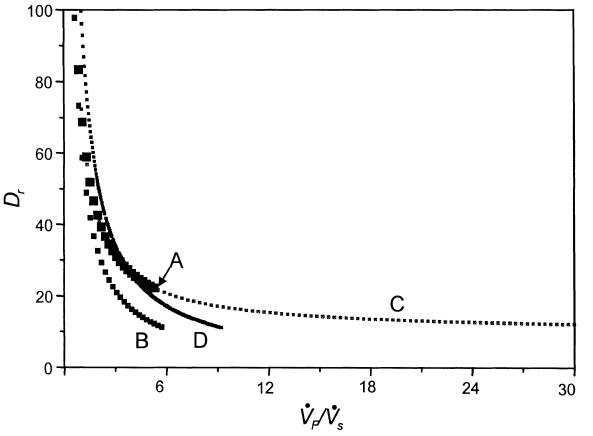

Fig. 18. Parameter D_r (quantifying the relative desorbent consumption, Eq. (51)) as a function of the feed flow-rate for typical separation regions determined with different strategies. $\bar{C}_{mod} = 10\%$, $C_{mod,F} = 0\%$, $C_F = 1\%$, $N^{I} = N^{II} = N^{III} = N^{IV} = 100$, $Pu_{1,R} > 95\%$, $Pu_{2,E} > 95\%$. (A) Isocratic (Fig. 9, region A); (B) strategy 3B (Fig. 9, region B); (C) strategy 3C (Fig. 11, region C), only a part of the dependence is shown; (D) strategy 3D (Fig. 14, region C).

10 and 12, for strategy 3D an increase of the feed flow-rate also causes an increases in the difference between the two internal modifier concentrations $C^{I,II}_{mod}$ and $C^{III,IV}_{mod}$. Instead of showing this, in Fig. 17, for region A from Fig. 16, the course of the equivalent safety factors β^{I} and β^{IV} as calculated from Eqs. (49) and (50) is depicted as a function of the feed flow-rate. In contrast to strategy 3C, the very attractive situation can now be observed that an increase of the feed flow-rate does not increase significantly or even lowers these safety factors and thus leads to reduced solvent consumption.

6.3. Comparison of desorbent consumption for the different strategies

Hitherto, mainly the productivity of the two-step gradient TMB (or SMB) process has been considered for the four different strategies 3A–3D related to the maximal differences between m^{III} and m^{II}. Also, the shape of the separation region with respect to their robust accessibility in a real process was discussed. To evaluate the potential of the process, of course the consumption of solvents is also important. A detailed analysis of this performance parameter is also outside the scope of this paper. Here, only the dimensionless parameter D_r, quantifying the relative consumption of the modifier, will be considered briefly:

$$D_r = \frac{\dot{V}_F C_{mod,F} + \dot{V}_D C_{mod,D}}{\dot{V}_F C_F} \tag{51}$$

To use the modifier economically this parameter should obviously be as small as possible. Fig. 18 shows selected D_r values for the four strategies based on fixing the averaged modifier concentration to $\bar{C}_{mod} = 10\%$. The parameter D_r is shown as a function of the feed flow-rate, which, for a productive process, should be as large as possible. It is evident that, for the isocratic mode (line A), the maximum achievable feed flow-rate is the lowest associated with the highest desorbent consumption at this point. Strategy 3B offers a marked improvement in terms of desorbent consumption, but it hardly enhances the process productivity. In contrast, based on strategy 3D, larger feed flow-rates can be processed for the same reduced modifier requirements. Analyzing the results shown in Fig. 18, strategy 3C appears to be the most attractive, since significantly higher feed flow-rates are applicable at the same low

desorbent consumption as for strategies 3B and 3D.

The results described above illustrate typical tendencies. Obviously, the two-step gradient process can be much superior compared to isocratic operation. However, no complete analysis of the effect of the different strategies on the related solvent requirements has been performed. In particular, the influence of isotherm nonlinearities, averaged modifier concentrations and purity requirements still needs to be studied more systematically.

7. Conclusion

In this work the two-step solvent gradient SMB process was analyzed numerically for linear equilibria. The results demonstrate the great potential of this concept. Various strategies for specifying suitable operating parameters were examined based on extensive numerical simulations. The most promising results were obtained when the average modifier concentration in the unit was fixed and the concentration of the modifier in the feed stream was set equal to zero. In order to avoid iterative solutions of the implicit problem, simpler explicit approaches have been suggested allowing us to calculate, in an efficient manner, suitable parameter regions. In particular, the approaches designated as strategies 3C and 3D appear to be attractive for identifying suitable operating conditions and will be analyzed further in the future. The presented results of the performed simulations hold, in principle, only for the particular parameter sets used in this work. Further systematic work needs to be done in order to draw more general conclusions. Fields that require a closer inspection are, for example, the impact of nonlinear equilibria and the fact that, often, modifier concentrations can be altered only in smaller regions.

Acknowledgements

Financial support of this work by Fonds der Chemischen Industrie and Schering AG is gratefully acknowledged.

References

[1] D.M. Ruthven, C.B. Ching, Chem. Eng. Sci. 44 (1989) 1011.
[2] P. Jandera, J. Churácek, Gradient Elution in Liquid Chromatography, Elsevier, Amsterdam, 1985.
[3] R.M. Nicoud, M. Perrut, G. Hotier, US Pat. 5 422 007, 1995.
[4] J.Y. Clavier, R.M. Nicoud, M. Perrut, in: High Pressure Chemical Engineering, Elsevier, London, 1995.
[5] M. Mazzotti, G. Storti, M. Morbidelli, J. Chromatogr. A 786 (1997) 309.
[6] N. Gottschlich, V. Kasche, J. Chromatogr. A 765 (1997) 201.
[7] C. Migliorini, M. Wendlinger, M. Mazzotti, M. Morbidelli, Ind. Eng. Chem. Res. 40 (2001) 2606.
[8] T.B. Jensen, T.G.P. Reijns, H.A.H. Billiet, L.A.M. van der Wielen, J. Chromatogr. A 873 (2000) 149.
[9] D. Antos, A. Seidel-Morgestern, Chem. Eng. Sci., in press.
[10] S. Abel, M. Mazzotti, M. Morbidelli, J. Chromatogr. A 944 (2002) 23.
[11] M. Mazzotti, G. Storti, M. Morbidelli, J. Chromatogr. A 769 (1997) 3.
[12] M. Mazzotti, G. Storti, M. Morbidelli, AIChE J. 47 (7) (2000) 1384.
[13] E. Soczewinski, Anal. Chem. 41 (1969) 179.
[14] D. Beltscheva, A. Seidel-Morgenstern, manuscript in preparation.